Isotope shift of the $1s2p\ ^3P_0$–$1s2s\ ^1S_0$ level splitting in heavy He-like ions: Implications for atomic parity-nonconservation studies

Fabrizio Ferro,[1,2,*] Anton Artemyev,[1,2] Thomas Stöhlker,[1,2,3] and Andrey Surzhykov[1,2]
[1]*Physikalisches Institut, Universität Heidelberg, Philosophenweg 12, D-69120 Heidelberg, Germany*
[2]*GSI Helmholtzzentrum für Schwerionenforschung, Planckstraße 1, D-64291 Darmstadt, Germany*
[3]*Helmholtz-Institut Jena, D-07743 Jena, Germany*
(Received 29 March 2010; published 7 June 2010)

Heavy He-like ions are considered to be promising candidates for atomic parity-nonconservation (PNC) studies, thanks to their relatively simple atomic structure and the significant mixing between the almost degenerate (for the atomic numbers $Z \sim 64$ and $Z \sim 91$) opposite-parity levels $1s2s\ ^1S_0$ and $1s2p\ ^3P_0$. A number of experiments exploiting this level mixing have been proposed, and their implementation requires a precise knowledge of the $2\ ^3P_0$–$2\ ^1S_0$ energy splitting for different nuclear charges and isotopes. In this paper we performed a theoretical analysis of the level splitting, employing the relativistic many-body perturbation theory and including QED corrections for all isotopes in the intervals $54 \leqslant Z \leqslant 71$ and $86 \leqslant Z \leqslant 93$. Possible candidates for future experimental PNC studies are discussed.

DOI: 10.1103/PhysRevA.81.062503 PACS number(s): 31.30.Gs, 31.15.am, 11.30.Er

I. INTRODUCTION

Parity-nonconservation (PNC) studies in atomic systems, stemming from the original proposal by Bouchiat and Bouchiat [1], have attained considerable interest both in experiments and theory [2]. Atomic PNC investigations are complementary to high-energy collider experiments insofar as they provide stringent tests of the standard model at low-momentum transfer. Up until the present, most atomic PNC experiments have been performed with neutral atoms. In particular, large parity-violating amplitudes were observed in forbidden transitions in ytterbium [3], while precise measurements with cesium beams [4] led to an accurate value of the weak nuclear charge Q_W in perfect agreement with the standard model [5,6].

The interpretation of the results of experiments with neutral atoms is hindered by the precision of atomic-structure calculations. Instead, in heavy highly charged ions electron-electron correlations are suppressed by a factor $1/Z$ with increasing atomic number Z. A theoretical treatment of few-body systems [7] [for example, making use of relativistic perturbation theory or multiconfiguration Dirac-Fock methods and including corrections of quantum electrodynamics (QED)] can nowadays achieve the required accuracy to extract PNC effects.

Heavy He-like ions are particularly envisaged for atomic PNC studies as was pointed out by Gorshkov and Labzovskii [8]. In fact, they are the simplest ions in which excited levels of opposite parity and equal total angular momentum get close in energy within certain intervals of the atomic number Z. In particular, the two levels $1s2s\ ^1S_0$ and $1s2p\ ^3P_0$ cross at $Z \sim 64$ and $Z \sim 91$. Moreover, they are characterized by a significant overlap between the electronic wave functions and the nucleus. Both these features enhance the PNC mixing between the two opposite-parity levels $1s2s\ ^1S_0$ and $1s2p\ ^3P_0$ that is described by the coefficient

$$i\eta = \frac{\langle \psi(2\ ^3P_0)|H_W|\psi(2\ ^1S_0)\rangle}{E(2\ ^1S_0) - E(2\ ^3P_0) + i\Gamma/2}, \qquad (1)$$

where Γ is the total width of the states.

Several proposals of PNC experiments exploit the near degeneracy of the states $1s2s\ ^1S_0$ and $1s2p\ ^3P_0$ in high-Z He-like ions and employ different techniques: laser-induced [9] or spontaneous [10] two-photon transitions, as well as radiative [11] or dielectronic recombination [12] in initially H-like ions. All proposed experiments require accurate calculations of the energy difference between the opposite-parity states.

Precise theoretical calculations of the $2\ ^3P_0$–$2\ ^1S_0$ energy splitting have been performed in recent years for a wide range of atomic numbers [13–17]. All these studies were done only for the most abundant isotope of a given Z. It is important, however, to also know the isotopic dependence of the $2\ ^3P_0$–$2\ ^1S_0$ splitting near the crossing points. In fact, the use of different isotopes may help to adjust the energy splitting to the needs of a particular experiment (e.g., in order to employ visible light to induce the two-photon electric-dipole $2E1$ transition between $1s2s\ ^1S_0$ and $1s2p\ ^3P_0$) and, moreover, will allow one to extract the weak charge Q_W [3] for neutrons and protons separately [18]. The isotopic dependence of the transition energy in uranium was partly considered only in Ref. [13]; nevertheless, the numerical uncertainty that resulted was too large.

On the ground of these motivations, we performed a systematic theoretical analysis of the $2\ ^3P_0$–$2\ ^1S_0$ energy splitting in He-like ions for several isotopes with atomic number Z in the intervals $54 \leqslant Z \leqslant 71$ and $86 \leqslant Z \leqslant 93$. In comparison to the most accurate results to date available in Ref. [17], we improved the treatment of electron correlations by applying a relativistic many-body perturbation theory (RMBPT) method to all orders and, in the important case of uranium, we adopted the most recent nuclear parameters in our calculations.

We will show that the isotopic dependence makes it possible to tune the energy splitting of the $1s2s\ ^1S_0$ and $1s2p\ ^3P_0$ levels within an interval of about ± 4 eV, and we discuss the implications on future PNC experiments with He-like ions.

The paper is organized as follows. In Sec. II we shall give a few details of the theoretical method. In Sec. III our results on the isotopic dependence of the $2\ ^3P_0$–$2\ ^1S_0$ energy splitting will be discussed, and the case of ^{238}U treated in detail. Conclusions will follow in Sec. IV.

*f.ferro@gsi.de

II. THEORETICAL TREATMENT OF THE $2\,^3P_0$–$2\,^1S_0$ ENERGY SPLITTING

A. Electron correlations

The $2\,^3P_0$–$2\,^1S_0$ energy splitting has been evaluated by separately treating electron correlations and QED corrections of the two levels $1s2s\,^1S_0$ and $1s2p\,^3P_0$. Electron correlations have been obtained using an all-order RMBPT method of two open-shell electrons [19] (see also Ref. [20] for an implementation of the method in nonrelativistic systems) that we shall briefly describe here.

We split the Hamiltonian H that describes a two-electron He-like ion as

$$H = H_0 + V, \tag{2}$$

where V accounts for electron correlations and H_0 is an independent-particle Hamiltonian that reads

$$H_0(\mathbf{r}_1,\mathbf{r}_2) = \bar{H}_0(\mathbf{r}_1) + \bar{H}_0(\mathbf{r}_2). \tag{3}$$

In Eq. (3), $\mathbf{r}_1$ and $\mathbf{r}_2$ are the positions of the electrons with respect to the nucleus, and

$$\bar{H}_0(\mathbf{r}_i) = H_D(\mathbf{r}_i) - Ze^2 \int_0^{+\infty} d\mathbf{r}' \frac{\rho_N(\mathbf{r}')}{|\mathbf{r}_i - \mathbf{r}'|}, \tag{4}$$

where H_D is the free-particle Dirac Hamiltonian and ρ_N is the charge distribution of the nucleus. The perturbation V contains both the Coulomb and Breit interactions between the two electrons ($1s$ and $2p_{1/2}$ or $1s$ and $2s$) on the same footing. The Breit term in the RMBPT is widely adopted to describe magnetic interactions and retardation effects [21]. No hyperfine interaction was considered here because both levels $1s2s\,^1S_0$ and $1s2p\,^3P_0$ have total angular momentum $J = 0$.

The aim of the RMBPT is to calculate perturbatively the energy spectrum E of the Hamiltonian H in Eq. (2). The Hamiltonian H_0 is discretized in a radial box and its two-electron eigenfunctions Φ_0 are evaluated numerically, as discussed, e.g., in Ref. [22]. A relativistic jj-coupling scheme is used here, since we are dealing with high-Z ions.

The problem is simplified by focusing on a subspace $\mathcal{P}$ (called model space), spanned by d eigenstates Φ_0^i of H_0 (with $i = 1,\ldots,d$): $\mathcal{P}$ is generally defined by including strongly mixing configurations, while all other configurations form an orthogonal space whose influence on the states of interest is accounted for in a perurbative way. In this work, in order to evaluate the energy level $1s2p\,^3P_0$ we chose a model space $\mathcal{P}$ that contains the two configurations $(1s2p_{1/2})J = 0$ and $(2s2p_{1/2})J = 0$, while for $1s2s\,^1S_0$ we chose solely the configuration $(1s2s_{1/2})J = 0$.

It is possible to establish a correspondence between d eigenfunctions Ψ^a of the full Hamiltonian H and their projections Ψ_0^a upon $\mathcal{P}$, called model functions,

$$\Psi_0^a = P\Psi^a \quad (a = 1,\ldots,d), \tag{5}$$

by using the the projection operator P that reads

$$P = \sum_{\Phi_0^i \in \mathcal{P}} |\Phi_0^i\rangle\langle\Phi_0^i|. \tag{6}$$

Under general conditions, Eq. (5) can be inverted, that is,

$$\Psi^a = \Omega\Psi_0^a \quad (a = 1,\ldots,d), \tag{7}$$

by making use of the wave operator Ω that satisfies the generalized Bloch equation [23,24]

$$[\Omega, H_0]P = V\Omega P - \Omega P V \Omega P. \tag{8}$$

From the eigenvalue equation of the full Hamiltonian H of the system,

$$H\Psi^a = E^a\Psi^a \quad (a = 1,\ldots,d), \tag{9}$$

and by employing Eq. (7) and operating with the projection operator P on both sides of Eq. (9), we can now define in $\mathcal{P}$ an effective Hamiltonian H^{eff} [23],

$$H^{\text{eff}} = PH_0P + PV\Omega P, \tag{10}$$

whose eigenvalue equation reads

$$H^{\text{eff}}\Psi_0^a = E^a\Psi_0^a \quad (a = 1,\ldots,d). \tag{11}$$

It follows from Eq. (11) that the eigenvalues of H^{eff} that correspond to the model functions Ψ_0^a are the exact energy eigenvalues E^a of the full Hamiltonian H that correspond to Ψ^a for $a = 1,\ldots,d$. In order to solve Eq. (11) and obtain the energies E^a, the wave operator Ω must be calculated from the Bloch equation (8). To reduce the complexity of this problem, in a perturbative approach Ω is expanded at nth order in a series

$$\Omega_n = I + \Omega^{(1)} + \cdots + \Omega^{(n)}, \tag{12}$$

where I is the identity operator. The generic term $\Omega^{(n)}$ contains n interactions with the perturbation V and follows recursively from the Bloch equation. With Ω_n, the nth order effective Hamiltonian $H_n^{\text{eff}} = PH_0P + PV\Omega_nP$ is defined, according to Eq. (10), and upon numerical diagonalization of H_n^{eff} one gets the exact energies E_n^a at nth order.

In the interval $54 \leqslant Z \leqslant 93$ considered in this work, we found that numerical convergence is achieved after just a few interactions.

B. Radiative corrections

The RMBPT method sketched in Sec. II A does not include radiative corrections. The latter are, however, important in heavy ions. Moreover, the accuracy that can be reached in experiments is of the same order as the size of the QED corrections, as shown, for example, in the recent measurement of the $1s2p_{3/2} \rightarrow 1s2s$ intrashell transition in He-like uranium [25]. In the past, the lack of sufficient accuracy in QED corrections hindered the calculation of level crossings (see, e.g., the discussion in Ref. [13]).

In the present work, we added QED corrections taken from recent literature to the eigenenergies E_n^a of the effective Hamiltonian in Eq. (10). In Ref. [17], *ab initio* calculations of two-electron QED effects to all orders in αZ in He-like ions were performed within the range $Z = 12$–100. From that paper we adopted the one-loop and the two-electron QED corrections. The two-loop QED correction is important for high-Z ions, since it scales as $(\alpha Z)^4\alpha^2$. Nevertheless, a precise evaluation of this term is only available for uranium and bismuth [26]. For other nuclides, we instead employed the numerical results of the two-loop correction from Ref. [17], which are the most accurate up to now. Higher-order [14] and

relativistic recoil corrections [27] have been also included in our final results.

III. RESULTS AND DISCUSSION

A. $2\,^3P_0$–$2\,^1S_0$ energy splitting in He-like ^{238}U ions

We shall discuss here in some detail our numerical results of the $1s2s\,^1S_0$ and $1s2p\,^3P_0$ energies in He-like ^{238}U, for the important role played by this nuclide, and as a test case of our method. A large source of theoretical uncertainty in the calculations of the energy levels lies in nuclear-size effects and in the nuclear model adopted. However, this can be reduced in the case of uranium, since a recent study of ^{238}U ions led to improved nuclear parameters for a deformed Fermi distribution [28].

References [28,29] discuss that the error produced by the choice of the nuclear model and of the nuclear deformation on the atomic energy levels is rather marginal, provided the correct rms nuclear radius is used. Therefore, since the RMBPT code that we are employing here was developed for spherical symmetry, we adopted in Eq. (4) a spherically symmetric Fermi radial distribution of the nuclear charge, with the rms radius $\langle r^2\rangle^{1/2} = 5.8569(33)$ fm recommended in Ref. [28]. Higher moments of the charge distribution were discarded.

The numerical uncertainty ε on the $2\,^3P_0$–$2\,^1S_0$ energy splitting in He-like ^{238}U was estimated by adding quadratically two different errors. The first one, $\varepsilon_{\rm rms}$, was obtained by varying the rms nuclear radius within its experimental uncertainty; the second one, $\varepsilon_{\rm distr.}$, was evaluated by calculating RMBPT correlations alternatively with a spherical and with a Fermi distribution of the nucleons. Our final estimate is $\varepsilon = \sqrt{\varepsilon_{\rm rms}^2 + \varepsilon_{\rm distr.}^2} = 0.131$ eV.

The numerical results of the $1s2s\,^1S_0$ and $1s2p\,^3P_0$ ionization energies in He-like ^{238}U ions are reported in Table I, while a comparison of the $2\,^3P_0$–$2\,^1S_0$ transition energy with previous results is given in Table II. Although the results of different authors are rather scattered, ours are in agreement, within the calculated error bars, with those of Maiorova *et al.* [11], Artemyev *et al.* [17], and Plante *et al.* [15].

TABLE II. Comparison of the $2\,^3P_0$–$2\,^1S_0$ transition energy in He-like ^{238}U ions (in chronological order) with previous calculations. All energies are in eV.

	$2\,^3P_0$–$2\,^1S_0$
This work	−2.793(131)
Maiorova *et al.* [11]	−2.81(8)
Artemyev *et al.* [17]	−2.64(28)
Andreev *et al.* [16]	−4.511
Maul *et al.* [13]	0.30
Plante *et al.* [15]	−2.6398
Drake [14]	−1.816

B. Isotopic dependence of the $2\,^3P_0$–$2\,^1S_0$ energy splitting

In order to explore the isotopic dependence of the $2\,^3P_0$–$2\,^1S_0$ energy splitting, extensive calculations have been performed for several isotopic chains of nuclei with atomic numbers close to $Z = 64$ and $Z = 91$ (i.e., where the $1s2s\,^1S_0$ and $1s2p\,^3P_0$ energy levels are expected to cross). Nuclides characterized by evanescent lifetimes were discarded, setting a limit of 10^{-3} s, because PNC experiments will be based on spectroscopy. RMBPT calculations of electron correlations have been performed separately at all orders for each (A,Z) combination, although only zeroth- and first-order terms make a significant contribution to the isotopic shift. The recoil correction has been taken into account according to each isotope mass. Owing to their relatively small value, QED corrections do not give any noticeable contribution to the isotope shift and may be kept fixed for each isotope.

For nuclides other than ^{238}U and ^{232}Th [for which, respectively, the recommended values $\langle r^2\rangle^{1/2} = 5.8569(33)$ [28] fm and $\langle r^2\rangle^{1/2} = 5.7210(613)$ fm [31] have been used], we adopted a spherical homogeneous nuclear distribution ρ_N in Eq. (4) with the rms nuclear radii listed in Ref. [32]. In

TABLE I. Contributions to the energies of the $1s2s\,^1S_0$ and $1s2p\,^3P_0$ states in He-like ^{238}U ions, relative to the ionization threshold. All energies are in eV.

	$1s2s\,^1S_0$	$1s2p\,^3P_0$
Dirac energy (pointlike nucleus)	−34 215.481	−34 215.4811
Nuclear size effects[a]	37.738	4.4133
Total zeroth-order energy	−34 177.743(27)	−34 211.0678(56)
First-order correlation [30]	850.135	923.198
Second-order correlation	−6.5368	−5.6726
Higher-order correlation	−0.0005	−0.0174
Total electron correlations	843.598(1)	917.508(4)
One-electron QED correction [26]	49.547(75)	6.846(12)
Two-electron QED correction [17]	−3.8259(4)	−4.4740(3)
Higher-order QED correction [14]	−0.009(51)	0.002(73)
Nuclear polarization and recoil correction [27]	0.0890	0.0491
Total energy	−33 288.344(94)	−33 291.137(74)

[a]A Fermi distribution for the nuclear charge with rms radius $\langle r^2\rangle^{1/2} = 5.8569(33)$ fm [28] was adopted.

the case of actinides ($86 \leqslant Z \leqslant 93$), for which the radius $R(N,Z)$ of a given isotope with Z protons and N neutrons is often unknown, we interpolated the reference radius R_0 of a neighboring nuclide with Z_0 protons and N_0 neutrons by employing the formula

$$R(N,Z) \approx R_0 \left(1 + \frac{\Delta N}{A_0}\right)^{k_Z} \left(1 + \frac{\Delta Z}{A_0}\right)^{k_N}, \qquad (13)$$

where $A_0 = Z_0 + N_0$, $\Delta Z = Z - Z_0$, and $\Delta N = N - N_0 \ll N$. Numerical values of the constants k_Z and k_N are 0.149(15) and 0.484(15), respectively [32].

The results are presented in Fig. 1 for the $54 \leqslant Z \leqslant 71$ interval (rare-earth metals) and in Fig. 2 for the $86 \leqslant Z \leqslant 93$ interval (actinides). Level crossings have been found in the $Z = 64$ isotopic chain of gadolinium between $A = 155$ and $A = 156$, and in the $Z = 91$ isotopic chain of protoactinium between $A = 219$ and $A = 220$.

According to Eq. (1), experiments on atomic parity-nonconservation will strongly profit from a close proximity of the two opposite-parity levels $1s2s\ ^1S_0$ and $1s2p\ ^3P_0$ since this enhances the PNC mixing. For these experiments, therefore, the ideal candidates are He-like protoactinium or gadolinium ions. We report numerical values of the $2\ ^3P_0$–$2\ ^1S_0$ energy splitting and lifetimes of the nuclides along the $Z = 64$ and $Z = 91$ chains in Table III. Results for $Z = 92$ are also listed because He-like uranium has been repeatedly proposed in the literature for PNC studies. The numerical uncertainties in Table III have been estimated by varying the radius of the nuclear distribution ρ_N within its experimental uncertainties.

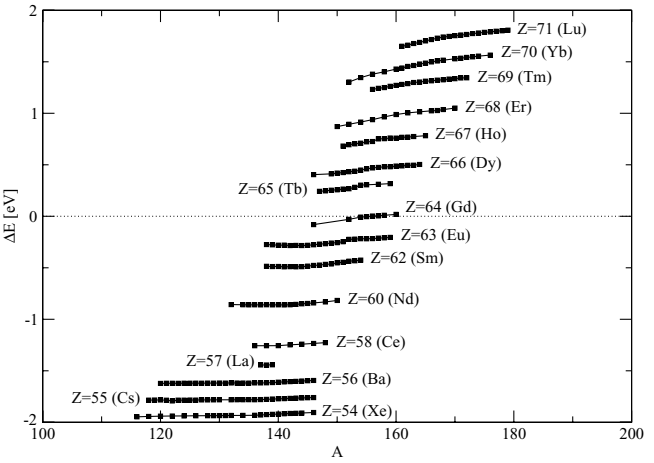

FIG. 1. Isotopic dependence of the $2\ ^3P_0$–$2\ ^1S_0$ energy splitting, ΔE, in He-like rare-earth-metal ions ($54 \leqslant Z \leqslant 71$). Solid lines connect nuclides of a given isotope chain. Solid squares represent nuclides for which an experimental rms nuclear radius is reported in the literature.

Some experimental schemes (e.g., those exploiting a $2E1$ laser-induced transition between the $1s2s\ ^1S_0$ and $1s2p\ ^3P_0$ levels) require that the level splitting is not exceedingly small because they can be best performed by employing methods of optical spectroscopy. If we consider Fig. 2, the transition energy for the $88 \leqslant Z \leqslant 92$ isotopic chains is confined between -3 and $+3$ eV: In order to employ these isotopes,

TABLE III. The $2\ ^3P_0$–$2\ ^1S_0$ energy splitting ΔE (in eV) along the isotopic chains of gadolinium ($Z = 64$), protoactinium ($Z = 91$), and uranium ($Z = 92$). The numerical uncertainties are, respectively, $\varepsilon_{\mathrm{Gd}} = 0.034$ eV, $\varepsilon_{\mathrm{Pa}} = 0.55$ eV, and $\varepsilon_{\mathrm{U}} = 0.27$ eV. Lifetimes were taken from Ref. [33].

Nuclide	ΔE	τ	Nuclide	ΔE	τ	Nuclide	ΔE	τ
^{146}Gd	−0.080	48.27 d	^{212}Pa	0.202	5.1 ms	^{218}U	−1.987	1.5 ms
^{152}Gd	−0.029	1.08×10^{14} yr	^{213}Pa	0.174	5.3 ms	^{224}U	−2.169	0.9 ms
^{154}Gd	−0.007	stable	^{214}Pa	0.147	17 ms	^{225}U	−2.199	95 ms
^{155}Gd	−0.003	stable	^{215}Pa	0.119	14 ms	^{226}U	−2.230	0.35 s
^{156}Gd	0.002	stable	^{216}Pa	0.091	0.20 s	^{227}U	−2.260	1.1 min
^{157}Gd	0.004	stable	^{217}Pa	0.064	4.9 ms	^{228}U	−2.290	9.1 min
^{158}Gd	0.009	stable	^{218}Pa	0.036	0.12 ms	^{229}U	−2.320	58 min
^{160}Gd	0.018	stable	^{222}Pa	−0.072	2.9 ms	^{230}U	−2.351	20.8 d
			^{223}Pa	−0.099	6.5 ms	^{231}U	−2.381	4.2 d
			^{224}Pa	−0.126	0.79 s	^{232}U	−2.411	68.9 yr
			^{225}Pa	−0.152	1.7 s	^{233}U	−2.442	1.592×10^5 yr
			^{226}Pa	−0.179	1.8 min	^{234}U	−2.565	2.455×10^5 yr
			^{227}Pa	−0.205	38.3 min	^{235}U	−2.563	7.038×10^8 yr
			^{228}Pa	−0.231	22 h	^{236}U	−2.628	2.342×10^7 yr
			^{229}Pa	−0.258	1.50 d	^{237}U	−2.658	6.75 d
			^{230}Pa	−0.284	17.4 d	^{238}U	−2.749	4.468×10^9 yr
			^{231}Pa	−0.310	32760 yr	^{239}U	−2.774	23.45 min
			^{232}Pa	−0.335	1.31 d	^{240}U	−2.804	14.1 h
			^{233}Pa	−0.440	26.967 d	^{242}U	−2.863	16.8 min
			^{234}Pa	−0.439	6.70 h			
			^{235}Pa	−0.495	24.5 min			
			^{236}Pa	−0.521	9.1 min			
			^{237}Pa	−0.596	8.7 min			
			^{238}Pa	−0.622	2.3 min			

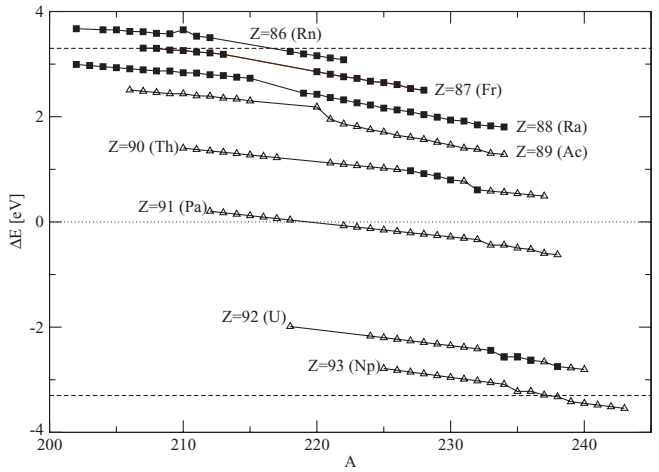

FIG. 2. Isotopic dependence of the $2\,^3P_0$–$2\,^1S_0$ transition splitting, ΔE, in He-like actinide ions ($86 \leqslant Z \leqslant 93$). Solid squares represent nuclides for which an experimental rms nuclear radius is reported in the literature, while triangles represent nuclides whose nuclear radius has been interpolated using Eq. (13). Solid lines connect nuclides of a given isotope chain. Horizontal dashed lines at ± 3.306 eV represent the limits for the use of visible photons in a $2E1$ transition between $2\,^3P_0$ and $2\,^1S_0$.

the two photons (each carrying half the transition energy) should accordingly have a wavelength smaller than 826.56 nm (i.e., in the infrared range). This situation, in principle, can be improved by using the Doppler shift in experiments performed at high-energy storage rings. Instead, optical photons may be used for $Z < 88$ and $Z > 92$. However, one might want to operate with high-Z ions in order to enhance PNC effects by increasing the overlap of the atomic wave functions with the nucleus. Therefore, suitable nuclides that allow employing optical photons are the isotopes of radon ($Z = 86$) with $A \lesssim 212$, the one isotope of francium ($Z = 87$) with $A = 207$, or the isotopes of neptunium ($Z = 93$) with $A \gtrsim 238$. Actually, neptunium is the only transuranic ion conceivable for PNC experiments since, for all heavier He-like ions, the $2\,^3P_0$–$2\,^1S_0$ energy splitting is rather large (e.g., -8.8 eV for ^{239}Pu), and therefore parity-violating effects are negligibly small due to the energy denominator in Eq. (1).

All actinide nuclides considered in this work are radioactive. Radon ions with $A \lesssim 212$ show very short lifetimes, reaching a maximum of 13 s for ^{212}Rn. A comparable lifetime of 14.8 s is offered by ^{207}Fr. The lifetimes of Np isotopes are instead of the order of days for $A = 238$ and $A = 239$, and decrease to a few minutes for $A = 240$. It is notable, however, that the ^{237}Np nuclide has a lifetime of 2.144×10^6 yr. Its transition energy is -3.290 eV and, as far as PNC experiments are concerned, photons of 753.7-nm wavelength would be required (i.e., at the border of the visible spectrum) in the near infrared. However, considering that PNC experiments with He-like ions will be performed at storage rings, ^{237}Np represents a suitable candidate since one could exploit the Doppler effect for a fine tuning of the photon frequency into the optical range.

Among the nuclides in the region of the crossing points, all protoactinium isotopes are radioactive with lifetimes of the order of milliseconds, while several gadolinium isotopes are stable or extremely long lived. The latter are therefore preferable for PNC spectroscopy.

IV. CONCLUSIONS

In this paper we presented a study of the $2\,^3P_0$–$2\,^1S_0$ energy splitting in He-like heavy ions in view of future experiments to measure PNC in atomic systems. We performed a systematic investigation of the transition energy upon the atomic number Z and the mass number A near the two crossings of the $1s2s\,^1S_0$ and $1s2p\,^3P_0$ levels at $Z = 64$ and $Z = 91$. Calculations were carried out employing a RMBPT method to all orders and including QED and recoil corrections from the literature. The isotopic dependence was introduced by varying the rms radius of the nuclear distribution ρ_N in Eq. (4). This allowed us to determine precisely that the crossing points of the $1s2s\,^1S_0$ and $1s2p\,^3P_0$ levels lie between the two isotopes ^{155}Gd and ^{156}Gd and between the isotopes ^{219}Pa and ^{220}Pa. Therefore, it is expected that PNC effects will be especially enhanced in He-like gadolinium and protoactinium ions.

In addition to the conditions of maximum PNC effects, we also discussed isotopes that can be used for spectroscopy of the $1s2s\,^1S_0$ and $1s2p\,^3P_0$ levels. The wavelengths of the photons required to induce the $2E1$ transition lie in the infrared range for most of the isotopic chains studied here. Nevertheless, a few radioactive nuclides belonging to the neptunium ($Z = 93$), francium ($Z = 87$), and radon ($Z = 86$) chains may be used and their He-like ions stimulated with visible photons. The lifetimes of actinides range from a few seconds to days. Nevertheless, the long-lived He-like ^{237}Np ion could be used with visible photons in storage rings that employ the Doppler effect and could be a candidate for PNC spectroscopy experiments.

ACKNOWLEDGMENTS

The authors gratefully acknowledge Professor V. M. Shabaev for providing the new rms radius of ^{232}Th and Dr. V. A. Yerokhin for valuable discussion on the two-loop QED correction. F. F. is indebted to Professor E. Lindroth for critical reading and useful comments on the manuscript. F. F., A. A., and A. S. acknowledge support from the Helmholtz association and GSI under Project No. VH-NG-421. The support by the ExtreMe Matter Institute EMMI in the framework of the Helmholtz Alliance HA216/EMMI is acknowledged.

[1] M. A. Bouchiat and C. Bouchiat, J. Phys. (Paris) **35**, 899 (1974); **36**, 493 (1975).

[2] J. S. M. Ginges and V. V. Flambaum, Phys. Rep. **397**, 63 (2004).

[3] K. Tsigutkin, D. Dounas-Frazer, A. Family, J. E. Stalnaker, V. V. Yashchuk, and D. Budker, Phys. Rev. Lett. **103**, 071601 (2009).

[4] C. S. Wood, S. C. Bennett, D. Cho, B. P. Masterson, J. L. Roberts, C. E. Tanner, and C. E. Wieman, Science **275**, 1759 (1997).
[5] S. C. Bennett and C. E. Wieman, Phys. Rev. Lett. **82**, 2484 (1999).
[6] S. G. Porsev, K. Beloy, and A. Derevianko, Phys. Rev. Lett. **102**, 181601 (2009).
[7] D. H. Sampson, H. Lin Zhang, and C. J. Fontes, Phys. Rep. **477**, 111 (2009).
[8] V. G. Gorshkov and L. I. Labzovski, ZhETF Pis. Red. **19**, 768 (1974); JETP Lett. **19**(12), 394 (1974).
[9] A. Schäfer, G. Soff, P. Indelicato, B. Müller, and W. Greiner, Phys. Rev. A **40**, 7362 (1989).
[10] R. W. Dunford, Phys. Rev. A **54**, 3820 (1996).
[11] A. V. Maiorova, O. I. Pavlova, V. M. Shabaev, C. Kozhuharov, G. Plunien, and T. Stöhlker, J. Phys. B **42**, 205002 (2009).
[12] G. F. Gribakin, F. J. Currell, M. G. Kozlov, and A. I. Mikhailov, Phys. Rev. A **72**, 032109 (2005).
[13] M. Maul, A. Schäfer, W. Greiner, and P. Indelicato, Phys. Rev. A **53**, 3915 (1996).
[14] G. W. F. Drake, Can. J. Phys. **66**, 586 (1988).
[15] D. R. Plante, W. R. Johnson, and J. Sapirstein, Phys. Rev. A **49**, 3519 (1994).
[16] O. Y. Andreev, L. N. Labzowsky, G. Plunien, and G. Soff, Phys. Rev. A **67**, 012503 (2003).
[17] A. N. Artemyev, V. M. Shabaev, V. A. Yerokhin, G. Plunien, and G. Soff, Phys. Rev. A **71**, 062104 (2005).
[18] E. N. Fortson, Y. Pang, and L. Wilets, Phys. Rev. Lett. **65**, 2857 (1990).
[19] S. Salomonson and P. Öster, Phys. Rev. A **40**, 5548 (1989).
[20] S. Salomonson and P. Öster, Phys. Rev. A **40**, 5559 (1989).
[21] E. Lindroth and J. Hvarfner, Phys. Rev. A **45**, 2771 (1992).
[22] M. Tokman, N. Eklöw, P. Glans, E. Lindroth, R. Schuch, G. Gwinner, D. Schwalm, A. Wolf, A. Hoffknecht, A. Müller, and S. Schippers, Phys. Rev. A **66**, 012703 (2002).
[23] I. Lindgren, J. Phys. B **7**, 2441 (1974).
[24] I. Lindgren and J. Morrison, *Atomic Many-Body Theory*, 2nd ed. (Springer-Verlag, Berlin, 1985).
[25] M. Trassinelli *et al.*, Eur. Phys. Lett. **87**, 63001 (2009).
[26] V. A. Yerokhin, P. Indelicato, and V. M. Shabaev, Phys. Rev. Lett. **97**, 253004 (2006).
[27] V. M. Shabaev and A. N. Artemyev, J. Phys. B **27**, 1307 (1994).
[28] Y. S. Kozhedub, O. V. Andreev, V. M. Shabaev, I. I. Tupitsyn, C. Brandau, C. Kozhuharov, G. Plunien, and T. Stöhlker, Phys. Rev. A **77**, 032501 (2008).
[29] W. R. Johnson and G. Soff, At. Data Nucl. Data Tables **33**, 405 (1985).
[30] A. N. Artemyev, T. Beier, G. Plunien, V. M. Shabaev, G. Soff, and V. A. Yerokhin, Phys. Rev. A **62**, 022116 (2000).
[31] Y. S. Kozhedub and V. M. Shabaev (private communication).
[32] I. Angeli, At. Data Nucl. Data Tables **87**, 185 (2004).
[33] S. Y. F. Chu, L. P. Ekström, and R. B. Firestone, The Lund/LBNL Nuclear Data Search [http://nucleardata.nuclear.lu.se/nucleardata/toi].